Ab Initio Determination of Optical Rotatory Dispersion in the Conformationally Flexible Molecule (*R*)-Epichlorohydrin

Mary C. Tam and T. Daniel Crawford*

Department of Chemistry, Virginia Tech, Blacksburg, Virginia 24061

Received: October 24, 2005; In Final Form: December 12, 2005

Ab initio optical rotation data from linear-response coupled-cluster and density-functional methods are compared to both gas-phase and liquid-phase polarimetry data for the small, conformationally flexible molecule epichlorohydrin. Three energy minima exist along the C−C−C−Cl dihedral angle, each with strong, antagonistic specific rotations ranging from ca. −450 to +500 deg/[dm (g/mL)] at 355 nm. Density-functional theory (specifically the B3LYP functional) consistently overestimates the optical rotations of each conformer relative to coupled-cluster theory (in agreement with our earlier observations for conformationally rigid species), and we attribute this to density-functional theory's underestimation of the lowest-lying excitation energies of epichlorohydrin. Length- and velocity-gauge formulations of the coupled-cluster response function lead to slightly different specific rotations (ca. 7% at short wavelengths). We have determined well-converged Gibbs free energy differences among the conformers using complete-basis-set extrapolations of coupled-cluster energies including triple excitations to obtain Boltzmann-averaged specific rotations for comparison to the gas-phase results. The length-gauge coupled-cluster data agree remarkably well with experiment, with the velocity-gauge coupled-cluster and density-functional data bracketing the experimental results from below and above, respectively. Liquid-phase conformer populations reported earlier by Polavarapu and co-workers from combined infrared absorption and theoretical analyses differ markedly from the gas-phase populations, particularly for polar solvents. Nevertheless, Boltzmann-averaged specific rotations from both coupled-cluster and density-functional calculations agree well with the corresponding experimental intrinsic rotations, although the theoretical specific rotations for the individual conformers do not take solvent effects into account. PCM-based estimates of conformer populations lead to poor agreement with experiment.

I. Introduction

Optical rotation, the rotation of plane-polarized light by samples of chiral species, occurs because such samples exhibit differing refractive indices for left- and right-circularly polarized light due to the dissymmetric electronic distributions inherent in chiral structures.[1,2] For decades organic chemists have sought a deeper understanding of the various factors influencing optical rotation due to its intimate connection to absolute configuration, a property of great interest to the pharmaceutical industry, for example. Ab initio calculation of optical rotation[3] is of relatively new interest, beginning with the work of Polavarapu in 1997 at the Hartree−Fock level of theory,[4] and since its implementation in density-functional theory (DFT)[5] in 2000,[6−11] and more recently in coupled-cluster (CC) theory,[7,12−16] it has been used successfully to determine the absolute configurations of a variety of molecules.[17,18] The development of ever more advanced theoretical techniques will improve our fundamental understanding of the relationship between molecular structure and optical rotation and help to design more robust tools for determining absolute configuration.[8,19,20]

For theoretical predictions of properties such as optical rotation to be reliable in the determination of the absolute configurations of chiral molecules, they must correctly predict both the sign and magnitude of the specific rotation [i.e., the total rotation, normalized for path length (dm) and concentration (g/mL)]. Such calculations naturally contain several "internal" sources of error, including those arising from truncation of the *N*-electron and one-electron spaces, electron correlation and basis-set effects, respectively, as well as difficulties arising from zero-point vibrational motion.[7,21−23] The comparison to experiment is further complicated by the wide variety of conditions under which optical rotation is measured in the laboratory, and "external" factors such as solvation and temperature provide strong perturbations in many cases.[24]

This work focuses specifically on the impact of conformational flexibility on theoretical determinations of optical rotation.[25−29] When several conformers are present in a given sample at a specified temperature, the observed specific rotation may be approximated as a weighted average of the rotations of the individual conformers. In 2003, Polavarapu et al. addressed this issue for the small molecule, (*R*)-epichlorohydrin, both by experiment and with DFT,[25] and obtained its intrinsic rotation (i.e., the limiting value of the specific rotation at zero concentration) in several solvents at 589 nm. Using the B3LYP[30,31] functional and a variety of basis sets, they found that the optical rotation varied greatly (and antagonistically) with the C−C−C−Cl dihedral angle among the three minimum-energy conformations, referred to as cis, gauche-I and gauche-II (Figure 1). Nevertheless, using conformer populations in several solvents (determined in a previous study,[32] where theoretical infrared absorption spectra were compared to those of experiment) and the B3LYP $[\alpha]_D$ values, they reported population-weighted specific rotations that compared reasonably well with the experimental solvent-phase data. For example, the observed

* Corresponding author. E-mail: crawdad@vt.edu.

10.1021/jp056093u CCC: $33.50
Published on Web 01/21/2006

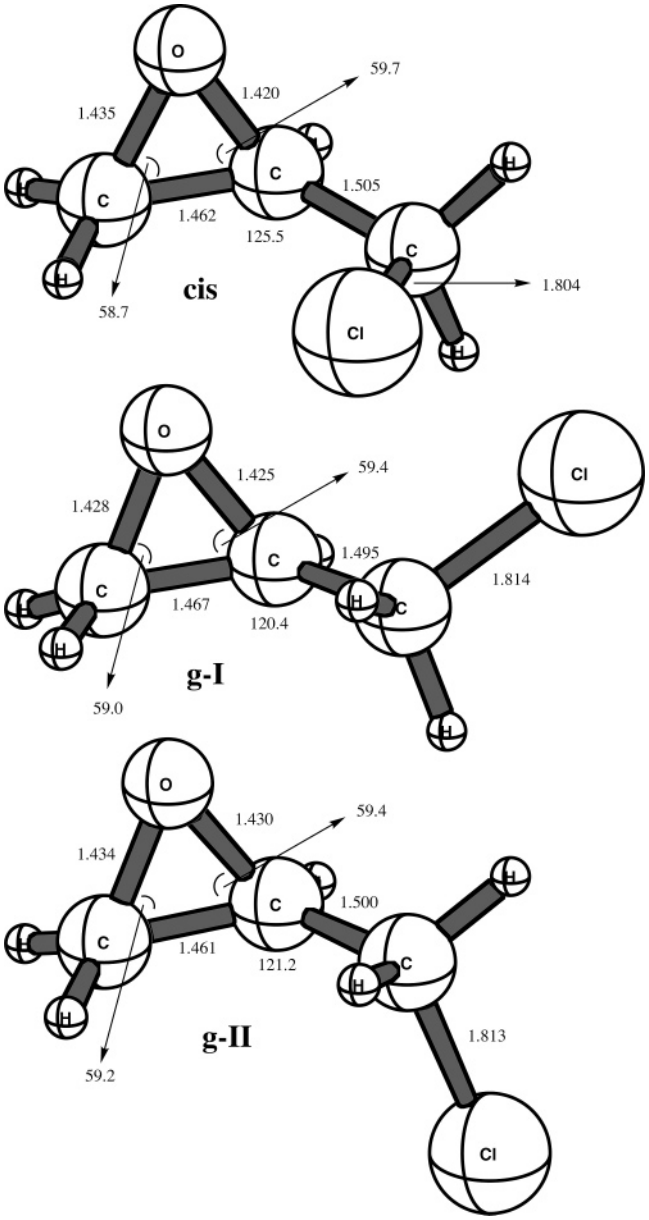

Figure 1. Optimized geometries of the three minimum-energy conformers (cis, gauche-I, and gauche-II) of (*R*)-epichlorohydrin at the B3LYP/cc-oVTZ level of theory. Bond lengths are given in Å, and bond angles in degrees.

intrinsic $[\alpha]_D$ for (*R*)-epichlorohydrin in $CHCl_3$ was $+3.2 \pm 1.5$ deg dm^{-1} (g/mL)$^{-1}$ as compared to the conformationally averaged B3LYP value of $+4 \pm 3$ deg dm^{-1} (g/mL)$^{-1}$. They further observed that corresponding shifts in conformer populations with solvent led to changes in both the magnitude and sign of the intrinsic rotation. In CH_2Cl_2, for example, the *g*-I conformer was found to be dominant with a mole fraction of 0.554 vs 0.345 for the *g*-II conformer, whereas in CCl_4 these values were reversed to 0.352 and 0.559, respectively. The changes in confomer populations with solvent explain the dramatic difference in intrinsic rotation: -22.4 ± 0.1 deg dm^{-1} (g/mL)$^{-1}$ in CH_2Cl_2 versus $+38.4 \pm 0.3$ deg dm^{-1} (g/mL)$^{-1}$ in CCl_4. Furthermore, the B3LYP values of $[\alpha]_D$ agreed reasonably well with experiment for each liquid-phase environment, although solvation effects were included only in the free energy and conformer population analysis and were ignored in the specific rotation calculations themselves.

The study by Polavarapu[25] left open two fundamental questions: (1) Are comparisons between the experimental condensed-phase data and (implicitly) gas-phase theoretical calculations robust? (2) How reliable is the time-dependent DFT (TD-DFT) B3LYP approach for optical rotation? That is, is the apparent success of DFT in the case of epichlorohydrin based on accurate rotations of the individual conformers or a providential averaging of inaccurate rotations?

Müller, Wiberg, and Vaccaro recently reported significant progress toward the answer to the first question with the development of the ultrasensitive cavity ring-down polarimetry (CRDP) technique, which has provided the first quantitative measurements of *gas-phase* optical rotation.[33,34] Since their initial publication of the details of such measurements, they have applied the CRDP approach to a number of small molecules, including epichlorohydrin, thus allowing more systematic comparisons between experiment and state-of-the-art theoretical models.[35,36] For the (*S*) enantiomer of epichlorohydrin, Wilson et al. recently reported specific rotations of -238.7 ± 2.3 deg dm^{-1} (g/mL)$^{-1}$ at 355 nm and -55.0 ± 1.7 deg dm^{-1} (g/mL)$^{-1}$ at 633 for a sample with 97% enantiomeric excess.[36] In addition, they carried out B3LYP-level DFT calculations in agreement with those reported earlier by Polavarapu[25] and explained the shifts in conformer populations in polar solvents such as acetonitrile on the basis of the widely differing dipole moments of the three conformers.

The purpose of this work is to address the second question regarding the reliability and accuracy of theoretical models of optical rotation when applied to conformationally flexible molecules. Specifically, we compare the new gas-phase CRDP data of Wilson et al. with results from both DFT and recently developed linear-response coupled-cluster methods.[7,12−14] Coupled-cluster theory is widely considered the most robust quantum chemical method for small molecules and has been used for hyperaccurate predictions of a variety of properties including geometrical structures, thermochemical data, vibrational spectra, UV/vis spectra, NMR spin−spin coupling constants, etc.[37−39] However, the overall dependability of coupled-cluster theory for response properties such as optical rotation remains an open question. Epichlorohydrin is an excellent test case for such questions, because it is small (with only five non-hydrogen atoms) and therefore allows the application of state-of-the-art computational methods.

II. Computational Details

In 1928, Rosenfeld developed the quantum mechanical foundations for first-principles calculations of optical rotation, and demonstrated that, for a nonabsorbing field of plane-polarized light of frequency ω, the angle of rotation, $[\alpha]_\omega$, of the light is related to the trace of the β tensor:[2,40,41]

$$\beta(\omega) = \frac{2}{\hbar} \mathrm{Im} \sum_{n \neq 0} \frac{\langle 0|\boldsymbol{\mu}|n\rangle\langle n|\mathbf{m}|0\rangle}{{\omega_{n0}}^2 - \omega^2} \qquad (1)$$

where $\boldsymbol{\mu}$ and $\mathbf{m}$ represent the electric- and magnetic-dipole operators, respectively, and the summation runs over all excited electronic (unperturbed) wave functions. In this work, we have computed β using the coupled-cluster singles and doubles (CCSD) linear response approach[14,42] to predict the optical rotation of the conformationally flexible chiral molecule (*R*)-ephchlorohydrin. For comparison, time-dependent density-functional theory (B3LYP)[5,31,30] with gauge invariant atomic orbitals (GIAOs)[43] was also used to calculate the optical rotation.[6,8,11,44] CCSD and B3LYP optical rotation calculations were carried out using several different basis sets: (1) the split

valence basis sets 6-31++G* and 6-311++G(2d,2p)[45] and (2) the correlation-consistent basis sets (aug-cc-pVDZ, aug-cc-pVTZ, and a mixed basis set denoted as "mixed-cc-pVTZ" which used the aug-cc-pVTZ basis set for carbon, oxygen, and chlorine and the cc-pVDZ basis set for hydrogen[46−49] using wavelengths of 355, 589, and 633 nm for each conformer). The coupled-cluster optical rotation calculations used both the length gauge (using the center of mass as the origin) and the "modified velocity gauge" (independent of origin) approach of Pedersen et al.[15] for the electric-dipole operator.

To account for conformational flexibility, we assume that the specific rotation can be expressed as a sum of the products of each individual conformer's optical rotation α_i and its corresponding mole fraction X_i:

$$\alpha_{AVG} = \alpha_A X_A + \alpha_B X_B + \alpha_C X_C + ... \quad (2)$$

where A refers to the lowest energy conformation and B, C, etc. refer to higher energy conformations. The X_i's for each conformation of (*R*)-epichlorohydrin are dependent upon the Gibbs free energies of the conformations

$$X_i = X_A \exp\left(\frac{-(G_i - G_A)}{RT}\right) \quad (3)$$

and X_A may be determined from $X_A + X_B + X_C + ... = 1$.

The individual conformations were identified using density-functional theory with the B3LYP functional. Each geometry was optimized and harmonic vibrational frequencies were computed for the cis, *g*-I, and *g*-II conformations of (*R*)-epichlorohydrin using Dunning's correlation-consistent cc-pVTZ basis set.[46]

Because the conformationally averaged theoretical optical rotation is highly dependent on the accuracy of the corresponding free energies, we employed several methods for a systematic comparison: B3LYP/cc-pVQZ, CCSD/cc-pVDZ, the composite methods, Gaussian-2 (G2)[50,51] and Gaussian-3 (G3)[52,53] theory, as well as complete-basis-set (CBS) extrapolations of coupled-cluster energies.[54,55] CBS extrapolations of the Hartree−Fock energy were carried out using the following equation,

$$E_X^{HF} = E_\infty^{HF} + Ae^{-BX} \quad (4)$$

where X is the cardinal number of the cc-pVXZ basis sets ($X = 2$ for cc-pVDZ, 3 for cc-pVTZ, etc.). The extrapolations of the correlation components of the frozen-core coupled-cluster energies were calculated using

$$E_X^{CC} = E_\infty^{CC} + AX^{-3} \quad (5)$$

The Hartree−Fock CBS extrapolations were carried out using the cc-pVDZ, cc-pVTZ, and cc-pVQZ basis sets whereas the coupled-cluster extrapolations used the cc-pVTZ and cc-pVQZ basis sets, the latter of which contains a total of 429 functions. The extrapolations were performed at the B3LYP/cc-pVTZ optimized geometry of each minimum-energy conformation. Harmonic vibrational frequencies were computed at the CCSD(T)/6-31G* level (using the corresponding optimized structure) to correct for zero-point energy and thermal effects (assuming the ideal gas/rigid rotor model).[56] Liquid-phase conformer populations were also obtained for several solvents (CH_2Cl_2, $CHCl_3$, CCl_4, and cyclohexane) at the B3LYP/cc-pVQZ level of theory using the polarizable continuum model (PCM)[57] to obtain internal energies, with the same CCSD(T)/6-31G* vibrational/thermal corrections used for the CBS-CC gas-phase populations.

Vertical electronic transition energies were computed using both equation-of-motion CCSD (EOM-CCSD)[58] and TD-DFT/B3LYP[59−61] approaches. All electrons were correlated for the geometry and vibrational frequency calculations, whereas core electrons (1s for C and Cl) were frozen for single point energies, excitation energies, and CCSD optical rotation calculations (except for the CCSD/mixed-cc-pVTZ optical rotation calculations where the core electrons, 1s for C and 1s2s2p for Cl, were frozen due to memory constraints). Both length-gauge and velocity-gauge CCSD optical rotation calculations were carried out to test the significance of freezing the core electrons. For each wavelength, our results indicate that freezing the 1s2s2p electrons for Cl has little impact on the computed rotation. At the CCSD/aug-cc-pVDZ level of theory, the specific rotations computed when freezing only the 1s electrons for Cl differ by less than 0.5 deg dm^{-1} $(g/mL)^{-1}$ from values computed at the same level of theory where the 1s2s2p core electrons of Cl were frozen. Gaussian03[62] was used for all B3LYP optimized geometries and optical rotation calculations. All coupled-cluster single point energies and optical rotation calculations were performed using the PSI3 program package.[63] CCSD(T) geometry optimizations and vibrational frequency calculations were carried out using Aces2.[64]

III. Results and Discussion

The B3LYP/cc-pVTZ optimized geometries of the three minimum-energy conformations of (*R*)-epichlorohydrin are reported in Figure 1. Apart from the C−C−C−Cl dihedral angle, most of the structural parameters of the three conformations vary only slightly. The conformations are denoted as cis, *g*-I, and *g*-II with dihedral angles of −20.6°, −151.1°, and 94.0°, respectively, in agreement with earlier studies.[32] The lowest energy gas-phase conformation is the *g*-II structure, with the *g*-I and cis conformers somewhat higher in energy, at approximately 0.5 and 1.6 kcal/mol, respectively.

Tables 1−3 summarize the computed values of individual conformer specific rotations in deg dm^{-1} $(g/mL)^{-1}$ using a variety of basis sets at the B3LYP and CCSD levels of theory, using wavelengths of plane-polarized light of 355, 589, and 633 nm, respectively. For each wavelength, the cis and *g*-II conformations give positive values of $[\alpha]_\lambda$, whereas the *g*-I conformer gives a negative rotation. The specific rotation of the cis conformer is the least dependent on the choice of basis set, whereas the $[\alpha]_\lambda$'s for the *g*-I and *g*-II conformers show significant variation, especially between the split valence and correlation consistent basis sets. We also see that the variation between basis sets decreases for each individual conformation as the choice of wavelength increases. For each of the conformers, $[\alpha]_\lambda$ deviates very little between the aug-cc-pVDZ and mixed-cc-pVTZ basis sets for each method, suggesting that the smaller correlation consistent basis set is reasonably well converged for this property. Also, the B3LYP calculations show almost no variation of $[\alpha]_\lambda$ between the mixed-cc-pVTZ and aug-cc-pVTZ basis sets, which suggests that the lack of diffuse functions on hydrogen has a negligible effect on the computed optical rotation. It can also be seen from Tables 1−3 that B3LYP consistently predicts optical rotation values which are much larger in magnitude than their CCSD counterparts for all of the basis sets and wavelengths used in this study and that the value of $[\alpha]_\lambda$ increases with decreasing wavelength.

Tables 1−3 report CCSD-level specific rotations for two choices of gauge for the electric-dipole operator: the origin-

TABLE 1: Specific Rotations (in deg/[dm (g/cm^3)]) of (*R*)-Epichlorohydrin Conformers at 355 nm[a]

conformation	6-31++G*	6-311++G(2d,2p)	aug-cc-pVDZ	mixed-cc-pVTZ[b]	aug-cc-pVTZ
			B3LYP		
cis	301.7	282.3	277.0	279.2	278.8
g-II	625.5	633.1	608.4	608.5	600.3
g-I	−659.7	−574.3	−513.6	−491.9	−493.2
			CCSD (Length Gauge)[c]		
cis	123.8	177.6	165.5	164.8	
g-II	520.0	559.4	499.6	508.3	
g-I	−563.5	−493.0	−436.1	−442.8	
			CCSD (Modified Velocity Gauge)		
cis	203.6	176.7	171.0	177.1	
g-II	422.5	504.5	438.0	473.3	
g-I	−481.7	−484.4	−392.3	−412.9	

[a] Computed at the B3LYP/cc-pVTZ optimized geometry. [b] aug-cc-pVTZ(C,O,Cl)+cc-pVDZ(H). [c] The center of mass was used as the coordinate origin.

TABLE 2: Specific Rotations (in deg/[dm (g/cm^3)]) of (*R*)-Epichlorohydrin Conformers at 589 nm[a]

conformation	6-31++G*	6-311++G(2d,2p)	aug-cc-pVDZ	mixed-cc-pVTZ[b]	aug-cc-pVTZ
			B3LYP		
g-cis	72.5	66.5	63.0	64.9	64.7
g-II	177.9	179.3	172.1	171.5	169.5
g-I	−216.9	−187.3	−167.8	−159.7	−160.2
			CCSD (Length Gauge)[c]		
cis	25.1	44.7	38.9	40.6	
g-II	153.2	167.2	146.5	149.9	
g-I	−187.1	−163.9	−145.0	−146.0	
			CCSD (Modified Velocity Gauge)		
cis	52.4	44.6	41.0	43.2	
g-II	124.1	149.9	127.2	139.2	
g-I	−162.1	−162.4	−131.8	−137.3	

[a] Computed at the B3LYP/cc-pVTZ optimized geometry. [b] aug-cc-pVTZ(C,O,Cl)+cc-pVDZ(H). [c] The center of mass was used as the coordinate origin.

TABLE 3: Specific Rotations (in deg/[dm (g/cm^3)]) of (*R*)-Epichlorohydrin Conformers at 633 nm[a]

conformation	6-31++G*	6-311++G(2d,2p)	aug-cc-pVDZ	mixed-cc-pVTZ[b]	aug-cc-pVTZ
			B3LYP		
cis	60.9	55.8	52.7	54.4	54.2
g-II	151.2	152.5	146.4	145.9	144.1
g-I	−186.4	−160.8	−144.0	−137.1	−137.5
			CCSD (Length Gauge)[c]		
cis	20.7	37.7	32.5	34.2	
g-II	130.8	142.7	124.9	127.9	
g-I	−160.9	−141.0	−124.6	−125.5	
			CCSD (Modified Velocity Gauge)		
cis	44.2	37.6	34.4	36.3	
g-II	105.8	128.0	108.4	118.7	
g-I	−139.6	−139.8	−113.4	−118.1	

[a] Computed at the B3LYP/cc-pVTZ optimized geometry. [b] aug-cc-pVTZ(C,O,Cl)+cc-pVDZ(H). [c] The center of mass was used as the coordinate origin.

dependent length-gauge representation and the origin-independent modified velocity-gauge representation of Pedersen et al.[15] For the latter, we have shifted the raw velocity-gauge rotation by its zero-frequency counterpart to account for the fact that this choice of gauge does not lead to the physically realistic result of $[\alpha]_\lambda = 0$ as $\lambda \rightarrow \infty$. As can be seen from the tables, the choice of length gauge vs velocity gauge has a significant impact on the coupled-cluster specific rotations, particularly for shorter wavelengths. At 355 nm, the mixed-cc-pVTZ basis CCSD rotation for *g*-II, for example, varies from 508.3 in the length gauge to 473.3 in the velocity gauge. This variation is much smaller for longer wavelengths but is nevertheless significant. The likely reason for this variation is the expected slower basis-set convergence of the velocity-gauge representation of the electric-dipole operator, though we note that, for coupled-cluster methods, the two representations will not give identical results even in the limit of a complete basis set.[3,65] Though both length- and velocity-gauge CCSD specific rotations are in semiquantitative agreement with each other, both are significantly lower than the corresponding B3LYP rotations. Further study of the comparative behavior of the length- and velocity-gauge representations is clearly needed.

The differences between the B3LYP and CCSD specific rotations can be understood in terms of the relative abilities of the two methods to predict accurately the lowest-lying excitation energies that implicitly influence the computed optical rotation via eq 1. Table 4 summarizes the lowest vertical excitation energies for each of the three minimum-energy conformers of (*R*)-epichlorohydrin using equation-of-motion CCSD (EOM-CCSD) and TD-DFT/B3LYP. The energies vary only slightly among the individual conformers, but comparison between the EOM-CCSD and TD-DFT methods shows more dramatic

TABLE 4: EOM-CCSD and B3LYP-TDDFT Excitation Energies for (*R*)-Epichlorohydrin Computed with Various Basis Sets at the B3LYP/cc-pVTZ Optimized Geometry

	individual conformer vertical excitation energies											
	EOM-CCSD						B3LYP/TDDFT					
	cc-pVTZ		aug-cc-pVDZ		6-311++G(2d,2p)		cc-pVTZ		aug-cc-pVDZ		6-311++G(2d,2p)	
conformation	eV	nm	eV	nm	eV	nm	eV	nm	eV	nm	eV	nm
cis	7.55	164	7.38	168	7.34	169	6.91	179	6.63	187	6.62	187
g-II	7.53	167	7.35	169	7.33	169	6.90	180	6.68	186	6.66	186
g-I	7.46	166	7.30	170	7.28	170	6.85	181	6.84	181	6.57	189

TABLE 5: Gas-Phase Conformer Populations of (*R*)-Epichlorohydrin

conformation	G2	G3	B3LYP/cc-pVQZ[a]	CBS CCSD[a]	CBS CCSD(T)[a]
g-cis	0.055	0.073	0.034	0.059	0.064
g-II	0.708	0.682	0.648	0.670	0.676
g-I	0.237	0.245	0.318	0.271	0.259

[a] Determined from Gibbs free energies based on internal energies at the given level of theory plus CCSD(T)/6-31G* vibrational/thermal corrections.

TABLE 6: Liquid-Phase Conformer Populations for (*R*)-Epichlorohydrin

	neat	CH_2Cl_2		$CHCl_3$		CCl_4		cyclohexane
conformation	expt[a]	B3LYP[b]	expt[a]	B3LYP[b]	expt[a]	B3LYP[b]	expt[a]	B3LYP[b]
cis	0.114	0.043	0.111	0.041	0.108	0.044	0.089	0.038
g-II	0.330	0.342	0.345	0.406	0.432	0.515	0.559	0.529
g-I	0.556	0.615	0.544	0.553	0.460	0.441	0.352	0.433

[a] Reference 25. [b] Determined from Gibbs free energies based B3LYP/cc-pVQZ internal energies including PCM corrections plus CCSD(T)/6-31G* vibrational/thermal corrections.

differences, with the latter falling below the former by approximately 0.7 eV. According to the gas-phase electronic circular dichroism (CD) spectrum measured by Basil et al. in 1991,[66] the lowest electronic excitation produces a positive CD band peaked at ca. 171.0 nm (7.25 eV), corresponding to a *n*(O) → 3s Rydberg excitation.

This peak falls 0.03−0.13 eV below the corresponding EOM-CCSD vertical excitation energy (depending on the conformer and using the aug-cc-pVDZ and 6-311++G(2d,2p) basis-sets), but 0.41−0.68 eV above the B3LYP results (again depending on the conformer and with the same basis sets). Given that the computed optical rotation is inversely proportional to the difference in the squares of the excitation energy and chosen frequency of plane polarized light (cf. eq 1), the consistent underestimation of vertical excitation energies by the B3LYP method leads to a concomitant overestimation of each conformer's $[\alpha]_\lambda$. (In addition, we note that B3LYP/aug-cc-pVDZ calculations indicate that this state is likely the major contributor to the measured gas-phase specific rotation with a rotational strength of ca. 11.3×10^{-40} cgs units.) This effect was also observed in (*S*)-methyloxirane[14] and (*P*)-[4]triangulane.[13] On the other hand, the agreement between the EOM-CCSD excitation energies and experiment suggests greater reliability of the CCSD optical rotation values. We note, however, the theoretical specific rotations reported here are not yet converged in that the level of electron correlation remains limited to double excitations at most, and other effects such as zero-point vibrational motion have been ignored.[21,22]

An opposing example, however, is given by (1*S*,4*S*)-norbornenone, for which CCSD (length gauge) and B3LYP specific rotations differ dramatically at −741 and −1216 deg/[dm (g/mL)], respectively, with only the latter in reasonable agreement with the liquid-phase experimental value of ca. −1150 deg/[dm (g/mL)]. As Ruud et al. demonstrated, the B3LYP values of both the lowest excitation energy and its rotational strength agree well with experiment in this case, whereas the corresponding CCSD values are too large and too small, respectively.[12] However, the norbornenone case differs from that of epichlorohydrin in that its lowest excited state arises from a valence $n \rightarrow \pi^*$ excitation, a type of transition often well-reproduced by the B3LYP functional, as opposed to the low-lying Rydberg transitions in epichlorohydrin. In addition, the comparison between theoretical gas-phase and experimental liquid-phase specific rotations is problematic, as demonstrated below.

Table 5 reports conformer populations for the gas phase using B3LYP, G2, G3, and CBS-extrapolated CC methods. In the gas phase the *g*-II conformation clearly dominates at 67−70%, followed by the *g*-I conformer at 24−27%, and finally the cis conformer at only about 5−7%. Note, however, that the gas-phase mole fractions vary only slightly with the level of theory, ±3% at most. Table 6 reports conformer populations for liquid-phase environments, including the neat state, methylenechloride, chloroform, carbon tetrachloride, and cyclohexane. The experimental data from ref 25 were determined using comparisons between experimental infrared absorption spectra in several solvent environments with their theoretical counterparts (B3LYP/aug-cc-pVTZ). The theoretical liquid-phase populations were obtained at the B3LYP/cc-pVQZ level of theory, including PCM-based solvent corrections. For each solvent in Table 6, the *g*-I conformation clearly dominates with the exception of CCl_4 and cyclohexane, for which conformer *g*-II lies lower in energy, as in the gas phase. These data are also consistent with the more recent results of Wilson et al., who observed a reversal of the sign of $[\alpha]_D$ in acetonitrile relative to the gas phase.[36] Clearly the solvent introduces significant perturbations to the system. However, the theoretical (B3LYP) populations are shifted significantly from the experimentally inferred values of Polavarapu et al.:[25] B3LYP tends to underestimate the population of the cis conformer relative to experiment (up to 6.8% for methylene chloride), and simultaneously overestimate that of the *g*-I conformer (up to 9.3% for chloroform).

Tables 7−9 summarize the B3LYP and CCSD specific rotations for (*R*)-epichlorohydrin at 355, 589, and 633 nm,

TABLE 7: Specific Rotations (in deg/[dm (g/cm^3)]) for (*R*)-Epichlorohydrin at 355 nm in Gas- and Liquid-Phase Environments[a]

			6-31++G*	6-311++G(2d,2p)	aug-cc-pVDZ	mixed-cc-pVTZ[b]	aug-cc-pVTZ
				B3LYP			
gas phase[c]	G2		303.0	327.5	324.1	329.5	323.3
	G3		286.8	311.5	309.1	314.7	308.7
	CBS CCSD(T)		272.1	298.0	296.7	302.5	296.6
liquid phase[d]	neat		−126.0	−78.2	−53.2	−40.9	−44.4
	CH_2Cl_2	expt	−109.6	−62.7	−38.8	−26.7	−30.3
		B3LYP	−179.2	−124.9	−96.2	−86.4	−82.7
	$CHCl_3$	expt	−0.65	39.8	56.5	66.8	62.5
		B3LYP	−98.0	−48.5	−25.2	−17.2	−13.1
	CCl_4	expt	144.3	176.9	184.0	191.9	186.8
		B3LYP	44.5	85.2	99.0	103.9	108.7
	cyclohexane		56.1	96.4	109.4	114.0	119.0
				CCSD (Length Gauge)[e]			
gas phase[c]	G2		241.3	288.8	259.4	263.9	
	G3		225.4	273.4	245.8	250.0	
	CBS CCSD(T)		214.0	262.3	235.9	240.0	
liquid phase[d]	neat		−127.6	−76.1	−58.7	−59.7	
	CH_2Cl_2	expt	−113.4	−62.2	−46.5	−47.2	
		B3LYP	−163.7	−104.6	−90.5	−91.7	
	$CHCl_3$	expt	−21.2	27.6	33.1	33.7	
		B3LYP	−95.0	−37.9	−31.2	−31.3	
	CCl_4	expt	103.3	149.6	140.5	143.0	
		B3LYP	24.7	78.4	72.2	73.7	
	cyclohexane		35.2	88.7	81.3	83.0	
				CCSD (Modified Velocity Gauge)			
gas phase[c]	G2		196.0	251.7	226.4	246.9	
	G3		184.8	237.8	214.9	234.4	
	CBS CCSD(T)		174.4	227.2	205.9	224.8	
liquid phase[d]	neat		−105.2	−82.8	−54.1	−53.2	
	CH_2Cl_2	expt	−93.7	−70.0	−43.3	−41.7	
		B3LYP	−143.3	−118.2	−84.3	−84.7	
	$CHCl_3$	expt	−17.1	14.0	27.2	33.7	
		B3LYP	−86.1	−55.6	−31.8	−28.6	
	CCl_4	expt	84.7	127.0	122.0	135.0	
		B3LYP	14.1	53.7	60.1	69.4	
	cyclohexane		22.2	63.2	67.9	77.9	

[a] Computed at the B3LYP/cc-pVTZ optimized geometry. [b] aug-cc-pVTZ(C,O,Cl)+cc-pVDZ(H). [c] Using conformer populations from Table 5. [d] Using conformer populations from Table 6. [e] The center of mass was used as the coordinate origin.

respectively, averaged using the populations reported in Tables 5 and 6. The gas-phase average $[\alpha]_\lambda$ values exhibit the same trend as seen for the individual conformer optical rotation results, with the B3LYP values always significantly larger than the CCSD values (using both length and velocity gauge). For the liquid-phase results, however, this is no longer the case. In fact, at 355 nm, CCSD predicts [α]'s that are larger in magnitude than those of B3LYP, and at 589 and 633 nm, B3LYP and CCSD give similar rotations. These data also indicate that, at all wavelengths and basis sets used in this study, the CCSD length-gauge values for $[\alpha]_\lambda$ are somewhat larger than the CCSD velocity-gauge values.

Just as for the individual conformer rotations in Tables 1−3, correlation-consistent basis sets provide much more rapidly convergent rotations than the split-valence sets, suggesting that the latter may not be well-suited to describe this property. Also, our calculations do not show significant differences in $[\alpha]_\lambda$ between the aug-cc-pVDZ and mixed-cc-pVTZ basis sets for the B3LYP and CCSD (length gauge) methods individually. The velocity-gauge CCSD $[\alpha]_\lambda$'s appears to be somewhat more sensitive to the choice of basis set than its length-gauge counterpart, especially at 355 nm, where the difference in specific rotation between the two basis sets is approximately 20 deg dm^{-1} (g/mL)$^{-1}$ for each of the methods used to compute the free energy. At all wavelengths, the conformationally averaged B3LYP $[\alpha]_\lambda$ determined using the mixed-cc-pVTZ and aug-cc-pVTZ basis sets for both the gas and liquid phases are not significantly different, indicating that the use of the larger basis set on the hydrogen atoms is not necessary in this case.

The best comparisons with experiment for all wavelengths in the gas phase are given by the CCSD length-gauge data. At 355 nm, Wilson et al.'s gas-phase experimental value[36] of -238.7 ± 2.3 deg dm^{-1} (g/mL)$^{-1}$ for the (*S*) enantiomer agrees extremely well with the length-gauge CCSD/mixed-cc-pVTZ specific rotation of +240.0 deg dm^{-1} (g/mL)$^{-1}$ for the (*R*) enantiomer, computed with the populations obtained from complete-basis-set extrapolations of the CCSD(T) correlation energy. B3LYP optical rotations at 355 nm do not agree as well with the experimental value for any of the methods used, giving results that are too large by about 25%. The CCSD modified velocity-gauge gives values of $[\alpha]_\lambda$ that are closer to the experimental value than B3LYP but are still too low by about 15 deg dm^{-1} (g/mL)$^{-1}$ (6%). The same trend is found at 633 nm, where the length-gauge CCSD/mixed-cc-pVTZ specific rotation of +56.3 deg dm^{-1} (g/mL)$^{-1}$ for (*R*) compares well with the gas-phase optical rotation of -55.0 ± 1.7 deg dm^{-1} (g/mL)$^{-1}$ of Wilson et al. for (*S*).[36]

At 589 nm, the experimental specific rotation for (*R*)-epichlorohydrin is −41.94 deg dm^{-1} (g/mL)$^{-1}$ in neat liquid.[36] The conformationally averaged results calculated using the theoretical gas-phase conformer populations for every method and basis set fail to produce the correct sign of the rotation and drastically overestimate its magnitude by a factor of more than 2. Although this is clearly an apples-to-oranges comparison of

TABLE 8: Specific Rotations (in deg/[dm (g/cm^3)]) for (*R*)-Epichlorohydrin at 589 nm in Gas- and Liquid-Phase Environments[a]

			6-31++G*	6-311++G(2d,2p)	aug-cc-pVDZ	mixed-cc-pVTZ[b]	aug-cc-pVTZ
				B3LYP			
gas phase[c]	G2		78.5	86.1	85.5	87.1	85.5
	G2		78.5	86.1	85.5	87.1	85.5
	G3		73.4	81.1	80.8	82.5	81.0
	CBS CCSD(T)		68.9	77.1	77.1	78.9	77.4
liquid phase[d]	neat		−53.6	−37.4	−29.3	−24.8	−25.8
	CH_2Cl_2	expt	−48.6	−32.7	−24.9	−20.5	−21.5
		B3LYP	−69.6	−51.2	−41.7	−37.9	−36.9
	$CHCl_3$	expt	−15.1	−1.6	4.0	7.6	6.5
		B3LYP	−44.6	−27.9	−20.2	−17.0	−15.9
	CCl_4	expt	29.5	40.2	42.7	45.4	44.1
		B3LYP	−0.9	12.6	17.4	19.4	20.7
	cyclohexane		2.7	16.1	20.6	22.6	23.9
				CCSD (Length Gauge)[e]			
gas phase[c]	G2		65.5	81.9	71.4	73.8	
	G3		60.4	77.0	67.1	69.4	
	CBS CCSD(T)		56.9	73.6	64.1	66.3	
liquid phase[d]	neat		−50.6	−30.9	−27.8	−27.1	
	CH_2Cl_2	expt	−46.1	−26.5	−24.0	−23.2	
		B3LYP	−61.7	−41.8	−37.5	−36.9	
	$CHCl_3$	expt	−17.2	1.7	0.8	2.0	
		B3LYP	−40.1	−20.8	−19.0	−18.1	
	CCl_4	expt	22.0	39.7	34.3	36.0	
		B3LYP	−2.5	15.8	13.2	14.6	
′	cyclohexane		0.8	19.0	16.0	17.5	
				CCSD (Modified Velocity Gauge)			
gas phase[c]	G2		52.3	70.0	61.0	68.4	
	G3		48.7	65.6	57.4	64.4	
	CBS CCSD(T)		45.4	62.3	54.6	61.5	
liquid phase[d]	neat		−43.2	−35.8	−26.6	−25.5	
	CH_2Cl_2	expt	−39.6	−31.7	−23.3	−21.9	
		B3LYP	−55.1	−46.8	−35.9	−35.0	
	$CHCl_3$	expt	−15.3	−5.1	−1.3	1.7	
		B3LYP	−37.0	−27.0	−19.5	−17.5	
	CCl_4	expt	16.9	30.6	28.4	33.4	
		B3LYP	−5.3	7.5	9.2	13.1	
	cyclohexane		−2.7	10.5	11.6	15.7	

[a] Computed at the B3LYP/cc-pVTZ optimized geometry. [b] aug-cc-pVTZ(C,O,Cl)+cc-pVDZ(H). [c] Using conformer populations from Table 5. [d] Using conformer populations from Table 6. [e] The center of mass was used as the coordinate origin.

the experimental and theoretical optical rotation data because of the lack of solvation modeling in the latter, the difference between the two serves to emphasize the need to include the effect of the solvent at least in the determination of conformer populations to obtain reasonable comparison with conventional polarimetry data in many cases. In addition, it may be necessary to explicitly include the effect of the solvent on the response function itself, though that does not appear to be the case for epichlorohydrin.

The conformationally averaged B3LYP and CCSD optical rotation values for the various liquid-phase environments shown in Tables 7−9 were calculated using the theoretical individual conformer optical rotations and the conformer populations given in Table 6, as determined both by PCM-corrected theoretical calculations and by Polavarapu et al.[25] Polavarapu et al. reported intrinsic optical rotations of (*R*)-epichlorohydrin of −22.4 deg dm^{-1} (g/mL)$^{-1}$in CH_2Cl_2, +3.2 deg dm^{-1} (g/mL)$^{-1}$ in $CHCl_3$, and +38.5 deg dm^{-1} (g/mL)$^{-1}$ in CCl_4 at 589 nm for the (*R*) enantiomer.[25] Using the experimentally inferred populations, the length-gauge CCSD results from Table 8 reproduce these values to within ±2.0 deg/[dm (g/mL)]. The velocity-gauge CCSD results are similar in quality, whereas B3LYP brackets the experimental results vs CCSD but nevertheless gives a reasonable comparison. This indicates that, although the B3LYP specific rotations for the individual conformers may, in fact, be too large, the statistically averaged rotations can still agree well with experiment. Although the solvent was not considered in the calculation of the Rosenfeld tensors for the individual conformers, the averaged specific rotations compare extremely well to experiment.

On the other hand, conformer populations based on the PCM-corrected B3LYP/cc-pVQZ Gibbs free energies compare very poorly to experiment. In every case, the PCM-based average rotations are shifted toward more negative values, leading to underestimation of the positive CCl_4 rotation (e.g., by approximately a factor of 2 at 355 nm with CCSD), overestimation of the negative CH_2Cl_2 rotation (again, by approximately a factor of 2 at 355 nm with CCSD), and the incorrect sign of the $CHCl_3$ rotation. This failure appears to result primarily from the overestimation of the *g*-I conformer population by the PCM-based free energies in Table 6 noted above.

Wilson et al. have also reported extrapolated cyclohexane solution-phase data, obtained from the experimental optical rotatory dispersion curve ranging from 365 to 589 nm and then extrapolating to 355 and 633 nm, giving specific rotations of −167.7 deg dm^{-1} (g/mL)$^{-1}$ at 355 nm and −30.4 deg dm^{-1} (g/mL)$^{-1}$ at 633 nm for the (*S*) enantiomer of epichlorohydrin. The PCM-based rotations of the (*R*) enantiomer in cyclohexane given in Tables 1 and 3 are too small by a factor of 2 at the CCSD/mix-cc-pVTZ level of theory. By comparison to the chlorine-based solvents above, this most likely occurs because

TABLE 9: Specific Rotations (in deg/[dm (g/cm^3)]) for (*R*)-Epichlorohydrin at 633 nm in Gas- and Liquid-Phase Environments[a]

			6-31++G*	6-311++G(2d,2p)	aug-cc-pVDZ	mixed-cc-pVTZ[b]	aug-cc-pVTZ
				B3LYP			
gas phase[c]	G2		66.2	72.9	72.4	73.6	72.4
	G3		61.9	68.6	68.3	69.6	68.5
	CBS CCSD(T)		58.0	65.2	65.2	66.6	65.4
liquid phase[d]	neat		−46.8	−32.7	−25.8	−22.3	−22.7
	CH_2Cl_2	expt	−42.4	−28.7	−22.0	−18.6	−19.1
		B3LYP	−60.4	−44.4	−36.3	−33.0	−32.7
	$CHCl_3$	expt	−13.8	−2.1	2.7	5.5	4.9
		B3LYP	−39.0	−24.6	−18.0	−15.2	−14.7
	CCl_4	expt	24.4	33.6	35.8	37.9	37.0
		B3LYP	−1.6	10.1	14.2	16.0	16.7
	cyclohexane		1.5	13.0	16.9	18.6	19.4
				CCSD (Length Gauge)[e]			
gas phase[c]	G2		55.6	69.7	60.6	62.7	
	G3		51.3	65.5	57.0	58.9	
	CBS CCSD(T)		48.2	62.5	54.3	56.3	
liquid phase[d]	neat		−43.9	−27.0	−24.4	−23.7	
	CH_2Cl_2	expt	−40.1	−23.3	−21.1	−20.4	
		B3LYP	−53.4	−36.3	−32.6	−32.1	
	$CHCl_3$	expt	−15.3	0.9	0.1	1.2	
		B3LYP	−34.9	−18.3	−16.8	−16.0	
	CCl_4	exp	18.43	33.5	28.8	30.4	
		B3LYP	−2.7	13.0	10.8	12.0	
	cyclohexane		0.2	15.8	13.2	14.5	
				CCSD (Modified Velocity Gauge)			
gas phase[c]	G2		44.3	59.5	51.7	58.1	
	G3		41.2	55.7	48.6	54.7	
	CBS CCSD(T)		38.4	52.8	46.2	52.1	
liquid phase[d]	neat		−37.6	−31.2	−23.4	−22.3	
	CH_2Cl_2	expt	−34.5	−27.7	−20.5	−19.2	
		B3LYP	−47.8	−40.7	−31.3	−30.5	
	$CHCl_3$	expt	−13.7	−5.0	−1.6	0.9	
		B3LYP	−32.3	−23.7	−17.2	−15.5	
	CCl_4	expt	14.0	25.7	23.7	28.0	
		B3LYP	−5.1	5.9	7.3	10.7	
	cyclohexane		−2.9	8.5	9.4	12.9	

[a] Computed at the B3LYP/cc-pVTZ optimized geometry. [b] aug-cc-pVTZ(C,O,Cl)+cc-pVDZ(H). [c] Using conformer populations from Table 5. [d] Using conformer populations from Table 6. [e] The center of mass was used as the coordinate origin.

of overestimation of the contribution of the *g*-I conformer's negative rotation.

IV. Conclusions

In this study, we have reported theoretical conformationally averaged values of the optical rotation at several polarized-field wavelengths for (*R*)-epichlorohydrin using coupled-cluster and density-functional theory. At 355 and 633 nm, the CCSD/aug-cc-pVTZ level of theory (using the length-gauge representation of the electric-dipole operator and the cc-pVDZ basis set for hydrogen) does a remarkable job reproducing the gas-phase specific rotation reported by Wilson et al.[36] The corresponding velocity-gauge values underestimate the experimental gas-phase results at 355 and 633 nm by approximately 14 deg dm^{-1} (g/mL)$^{-1}$ (6%) and 3 deg dm^{-1} (g/mL)$^{-1}$ (5%), respectively. It remains unclear whether this is an instrinsic shortcoming of the "modified" velocity-gauge formulation[15] or simply the result of slower basis-set convergence relative to the length-gauge approach. The B3LYP method overestimates the specific rotation for both wavelengths: approximately 58 deg dm^{-1} (g/mL)$^{-1}$ (24%) at 355 nm and 10 deg dm^{-1} (g/mL)$^{-1}$ (19%) at 633 nm. As for our earlier studies of the conformationally rigid molecules (*S*)-methyloxirane and (*P*)-[4]triangulane, we have rationalized these errors on the basis of the concomitant underestimation of the lowest excitation energies of (*R*)-epichlorohydrin by the TD-DFT/B3LYP approach.

Comparison to the solution-phase experimental data of Polavarapu et al.[25] requires that solvent effects be considered in the Boltzmann averaging of the individual conformers. If this factor is ignored, then both B3LYP and coupled-cluster theories overestimate the magnitude of the conformationally averaged optical rotation by more than a factor of 2, and even fail to reproduce the correct sign at 589 nm. However, when solvent effects are incorporated via experimental estimates of the conformer populations, both CCSD and B3LYP give reasonable comparison to experimental sodium D-line specific (intrinsic) rotations, despite the rather large differences in rotations for each conformer between the two methods. On the other hand, PCM-based estimates of the conformer populations compare poorly to experiment in this case.

Acknowledgment. This work was supported by a National Science Foundation CAREER award (CHE-0133174), a New Faculty Award from the Camille and Henry Dreyfus Foundation, and a Cottrell Scholar Award from the Research Corporation. We are grateful to Mr. Shaun Wilson and Profs. Patrick Vaccaro and Kenneth Wiberg of Yale University for providing their gas-phase optical rotation data for epichlorohydrin in advance of publication.

References and Notes

(1) Charney, E. *The Molecular Basis of Optical Activity: Optical Rotatory Dispersion and Circular Dichroism*; John Wiley and Sons: New York, 1979.

(2) Barron, L. D. *Molecular Light Scattering and Optical Activity*, 2nd ed.; Cambridge University Press: Camridge, U.K., 2004.
(3) Crawford, T. D. *Theor. Chem. Acc.*, in press.
(4) Polavarapu, P. L. *Mol. Phys.* **1997**, *91* (3), 551−554.
(5) Parr, R. G.; Yang, W. *Density-Functional Theory of Atoms and Molecules*; Oxford University: New York, 1989.
(6) Cheeseman, J. R.; Frisch, M. J.; Devlin, F. J.; Stephens, P. J. *J. Phys. Chem. A* **2000**, *104*, 1039−1046.
(7) Ruud, K.; Helgaker, T. *Chem. Phys. Lett.* **2002**, *352*, 533−539.
(8) Stephens, P. J.; McCann, D. M.; Cheeseman, J. R.; Frisch, M. J. *Chirality* **2005**, *17*, S52−S64.
(9) Grimme, S. *Chem. Phys. Lett.* **2001**, *339*, 380−388.
(10) Stephens, P. J.; Devlin, F. J.; Cheeseman, J. R.; Frisch, M. J. *J. Phys. Chem. A* **2001**, *105* (22), 5356−5371.
(11) Autschbach, J.; Patchkovskii, S.; Ziegler, T.; van Gisbergen, S.; Baerends, E. J. *J. Chem. Phys.* **2002**, *117* (2), 581−592.
(12) Ruud, K.; Stephens, P. J.; Devlin, F. J.; Taylor, P. R.; Cheeseman, J. R.; Frisch, M. J. *Chem. Phys. Lett.* **2003**, *373*, 606−614.
(13) Crawford, T. D.; Owens, L. S.; Tam, M. C.; Schreiner, P. R.; Koch, H. *J. Am. Chem. Soc.* **2005**, *127*, 1368−1369.
(14) Tam, M. C.; Russ, N. J.; Crawford, T. D. *J. Chem. Phys.* **2004**, *121*, 3550−3557.
(15) Pedersen, T. B.; Koch, H.; Boman, L.; de Meras, A. M. J. S. *Chem. Phys. Lett.* **2004**, *393* (4−6), 319−326.
(16) Kongsted, J.; Pedersen, T. B.; Strange, M.; Osted, A.; Hansen, A. E.; Mikkelsen, K. V.; Pawlowski, F.; Jørgensen, P.; Hättig, C. *Chem. Phys. Lett.* **2005**, *401*, 385−392.
(17) Stephens, P. J.; Devlin, F. J.; Cheeseman, J. R.; Frisch, M. J.; Rosini, C. *Org. Lett.* **2002**, *4*, 4595−4598.
(18) Giorgio, E.; Viglione, R. G.; Zanasi, R.; Rosini, C. *J. Am. Chem. Soc.* **2004**, *126*, 12968−12976.
(19) Polavarapu, P. L. *Chirality* **2002**, *14*, 768−781.
(20) Stephens, P. J.; Devlin, F. J.; Cheeseman, J. R.; Drisch, M. J.; Bortolini, O.; Besse, P. *Chirality* **2003**, *15*, S57−S64.
(21) Ruud, K.; Zanasi, R. *Angew. Chem., Int. Ed. Engl.* **2005**, *44* (23), 3594−3596.
(22) Kongsted, J.; Pedersen, T. B.; Jensen, L.; Hansen, A. E.; Mikkelsen, K. V. *J. Am. Chem. Soc.*, in press.
(23) Mort, B. C.; Autschbach, J. *J. Phys. Chem. A* **2005**, *109* (38), 8617−8623.
(24) Kumata, Y.; Furukawa, J.; Fueno, T. *Bull. Chem. Soc. Jpn.* **1970**, *43*, 3 (12), 3920−3921.
(25) Polavarapu, P. L.; Petrovic, A.; Wang, F. *Chirality* **2003**, *15*, S143−S149.
(26) Wiberg, K. B.; Vaccaro, P. H.; Cheeseman, J. R. *J. Am. Chem. Soc.* **2003**, *125*, 1888−1896.
(27) Wiberg, K. B.; Wang, Y.-G.; Vaccaro, P. H.; Cheeseman, J. R.; Luderer, M. R. *J. Phys. Chem. A* **2005**, *109* (15), 3405−3410.
(28) Pecul, M.; Ruud, K.; Rizzo, A.; Helgaker, T. *J. Phys. Chem. A* **2004**, *108*, 4269−4276.
(29) Marchesan, D.; Coriani, S.; Forzato, C.; Nitti, P.; Pitacco, G.; Rudd, K. *J. Phys. Chem. A* **2005**, *109*, 1449−1453.
(30) Lee, C.; Yang, W.; Parr, R. G. *Phys. Rev. B.* **1988**, *37*, 785−789.
(31) Becke, A. D. *J. Chem. Phys.* **1993**, *98*, 5648−5652.
(32) Wang, F.; Polavarapu, P. L. *J. Phys. Chem. A* **2000**, *104*, 6189−6196.
(33) Müller, T.; Wiberg, K. B.; Vaccaro, P. H.; Cheeseman, J. R.; Frisch, M. J. *J. Opt. Soc. Am. B* **2002**, *19*, 125−141.
(34) Müller, T.; Wiberg, K. B.; Vaccaro, P. H. *J. Phys. Chem. A* **2000**, *104*, 5959−5968.
(35) Wiberg, K. B.; g. Wang, Y.; Wilson, S. M.; Vaccaro, P. H.; Cheeseman, J. R. *J. Phys. Chem. A* **2005**, *109* (15), 3448−3453.
(36) Wilson, S. M.; Wiberg, K. B.; Cheeseman, J. R.; Frisch, M. J.; Vaccaro, P. H. *J. Phys. Chem. A* **2005**, *109* (51), 11752−11764.
(37) Crawford, T. D.; Schaefer, H. F. In *Reviews in Computational Chemistry*; Lipkowitz, K. B., Boyd, D. B., Eds.; VCH Publishers: New York, 2000; Vol. 14, Chapter 2, pp 33−136.
(38) Bartlett, R. J. In *Modern Electronic Structure Theory*; Yarkony, D. R., Ed.; *Advanced Series in Physical Chemistry*, Vol. 2; World Scientific: Singapore, 1995; Chapter 16, pp 1047−1131.
(39) Lee, T. J.; Scuseria, G. E. In *Quantum Mechanical Electronic Structure Calculations with Chemical Accuracy*; Langhoff, S. R., Ed.; Kluwer Academic Publishers: Dordrecht, 1995; pp 47−108.
(40) Rosenfeld, L. *Z. Phys.* **1928**, *52*, 161.
(41) Caldwell, D. J.; Eyring, H. *The Theory of Optical Activity*; Wiley: New York, 1971.
(42) Koch, H.; Jørgensen, P. *J. Chem. Phys.* **1990**, *93* (5), 3333−3344.
(43) Ditchfield, R. *Mol. Phys.* **1974**, *27* (4), 789−807.
(44) Stephens, P. J.; Devlin, F. J. *Chirality* **2000**, *12*, 172−179.
(45) Pople, J. A. In *Energy, Structure, and Reactivity*; Smith, D. W., McRae, W. B., Eds.; John Wiley: New York, 1973; pp 51−61.
(46) Dunning, T. H. *J. Chem. Phys.* **1989**, *90* (2), 1007.
(47) Kendall, R. A.; Dunning, T. H.; Harrison, R. J. *J. Chem. Phys.* **1992**, *96* (9), 6796−6806.
(48) Woon, D. E.; Dunning, T. H. *J. Chem. Phys.* **1993**, *98* (2), 1358.
(49) Woon, D. E.; Dunning, T. H. *J. Chem. Phys.* **1994**, *100* (4), 2975.
(50) Curtiss, L. A.; Raghavachari, K.; Trucks, G. W.; Pople, J. A. *J. Chem. Phys.* **1991**, *94* (11), 7221.
(51) Curtiss, L. A.; Raghavachari, K.; Pople, J. A. *J. Chem. Phys.* **1995**, *103* (10), 4192.
(52) Curtiss, L. A.; Raghavachari, K.; Redfern, P. C.; Rassolov, V.; Pople, J. A. *J. Chem. Phys.* **1998**, *109*, 7764−7776.
(53) Curtiss, L. A.; Raghavachari, K. *Theor. Chem. Acc.* **2002**, *108*, 61−70.
(54) Feller, D. *J. Chem. Phys.* **1992**, *96* (8), 6104.
(55) Halkier, A.; Helgaker, T.; Jørgensen, P.; Klopper, W.; Koch, H.; Olsen, J.; Wilson, A. K. *Chem. Phys. Lett.* **1998**, *286* (3−4), 243.
(56) McQuarrie, D. A. *Statistical Thermodynamics*; University Science Books: Mill Valley, CA, 1973.
(57) Tomasi, J.; Cammi, R.; Mennucci, B.; Cappelli, C.; Corni, S. *Phys. Chem. Chem. Phys.* **2002**, *4*, 5697−5712.
(58) Stanton, J. F.; Bartlett, R. J. *J. Chem. Phys.* **1993**, *98* (9), 7029.
(59) Jamorski, C.; Casida, M. E.; Salahub, D. R. *J. Chem. Phys.* **1996**, *104* (13), 5134−5147.
(60) Bauernschmitt, R.; Ahlrichs, R. *Chem. Phys. Lett.* **1996**, *256* (4−5), 454−464.
(61) Casida, M. E.; World Scientific: Singapore, 1995; Vol. 1.
(62) Frisch, M. J.; Trucks, G. W.; Schlegel, H. B.; Scuseria, G. E.; Robb, M. A.; Cheeseman, J. R.; Montgomery, J. A.; Jr..; Vreven, T.; Kudin, K. N.; Burant, J. C.; Millam, J. M.; Iyengar, S. S.; Tomasi, J.; Barone, V.; Mennucci, B.; Cossi, M.; Scalmani, G.; Rega, N.; Petersson, G. A.; Nakatsuji, H.; Hada, M.; Ehara, M.; Toyota, K.; Fukuda, R.; Hasegawa, J.; Ishida, M.; Nakajima, T.; Honda, Y.; Kitao, O.; Nakai, H.; Klene, M.; Li, X.; Knox, J. E.; Hratchian, H. P.; Cross, J. B.; Adamo, C.; Jaramillo, J.; Gomperts, R.; Stratmann, R. E.; Yazyev, O.; Austin, A. J.; Cammi, R.; Pomelli, C.; Ochterski, J. W.; Ayala, P. Y.; Morokuma, K.; Voth, G. A.; Salvador, P.; Dannenberg, J. J.; Zakrzewski, V. G.; Dapprich, S.; Daniels, A. D.; Strain, M. C.; Farkas, O.; Malick, D. K.; Rabuck, A. D.; Raghavachari, K.; Foresman, J. B.; Ortiz, J. V.; Cui, Q.; Baboul, A. G.; Clifford, S.; Cioslowski, J.; Stefanov, B. B.; Liu, G.; Liashenko, A.; Piskorz, P.; Komaromi, I.; Martin, R. L.; Fox, D. J.; Keith, T.; Al-Laham, M. A.; Peng, C. Y.; Nanayakkara, A.; Challacombe, M.; Gill, P. M. W.; Johnson, B.; Chen, W.; Wong, M. W.; Gonzalez, C.; Pople, J. A. *Gaussian-03*; Gaussian, Inc.: Pittsburgh, PA, 2003.
(63) Crawford, T. D.; Sherrill, C. D.; Valeev, E. F.; Fermann, J. T.; King, R. A.; Leininger, M. L.; Brown, S. T.; Janssen, C. L.; Seidl, E. T.; Kenny, J. P.; Allen, W. D. *Psi 3.2*; 2003.
(64) Stanton, J. F.; Gauss, J.; Watts, J. D.; Lauderdale, W. J.; Bartlett, R. J. *ACES II*; 1993. The package also contains modified versions of the MOLECULE Gaussian integral program of J. Almlöf and P. R. Taylor, the ABACUS integral derivative program written by T. U. Helgaker, H. J. Aa. Jensen, P. Jørgensen and P. R. Taylor, and the PROPS property evaluation integral code of P. R. Taylor.
(65) Pedersen, T. B.; Koch, H.; Hättig, C. *J. Chem. Phys.* **1999**, *110* (17), 8318−8327.
(66) Basil, A.; Ben-Tzur, S.; Gedanken, A.; Rodger, A. *Chem. Phys. Lett.* **1991**, *180*, 482−484.